Progress towards a Refractive Real-Time MWIR Hyperspectral Imager

Brian Catanzaro[a], Mark Dombrowski[b], Paul Willson[c], Jeff Hendrixson[d], Eric Hillenbrand[d], John Wilcox[e]

[a] CFE Services, 5147 Pacifica Dr., San Diego, CA 92109[1]
[b] Surface Optics Corporation
[c] Picatinny Arsenal
[d] Naval Surface Warfare Center, Crane Division
[e] Wilcox Engineering

ABSTRACT

Hyperspectral imaging in the 2-5 um band has held interest for applications in detection and discrimination of targets. Real time instrumentation is particularly powerful as a tool for characterization and field measurement. A compact, real-time, refractive MWIR hyperspectral imaging instrument has been designed and is undergoing integration and test. The system has been designed for cryogenic operation to improve signal to noise ratio, reduce background noise, and enable real-time hyperspectral video processing. Partial testing has been completed on cryogenic elements and "first light" 2-5 μm hyperspectral images have been collected at room temperature.

Keywords: Hyperspectral imaging, MWIR, Slit based, Prism based, Cryogenic, Microbolometer, HgCdTe

1. REAL-TIME HYPERSPECTRAL IMAGING

Real-time imaging over broad bands in the electromagnetic spectrum from the ultraviolet (UV) through the infrared (IR) has been a staple in the areas of remote sensing, surveillance, target detection and tracking, search and homing devices, spectrally tailored coating development, nondestructive inspection, and noninvasive diagnosis. Improvements are being made in these techniques all the time, with increased resolution, higher sensitivity, and greater information throughput being the benefit. Instrumentation developed at Surface Optics has been used to distinguish objects based on their spectral signature in a number of applications. These include: revealing camouflaged military targets, friend-foe identification based on subtle coloring of personnel uniforms, and tracking of civilian vehicles based on spectral signature. [1,2]

2. SYSTEM ARCHITECTURE

The goals for a MWIR Hyperspectral Imager (MWIR HSI) under development at Surface Optics include:

- Operation over the MWIR spectrum: 2 – 5 μm
- Real time video data collection and processing: 15 hypercubes/sec
- Relatively rich spectrum: 30 bands
- Field deployable system

[1] Correspondence - Email: bcatanza@alumni.caltech.edu; Telephone: 858-204-6299

Infrared Technology and Applications XXX, edited by Bjørn F. Andresen, Gabor F. Fulop, Proc. of SPIE Vol. 5406 (SPIE, Bellingham, WA, 2004)
0277-786X/04/$15 · doi: 10.1117/12.543871

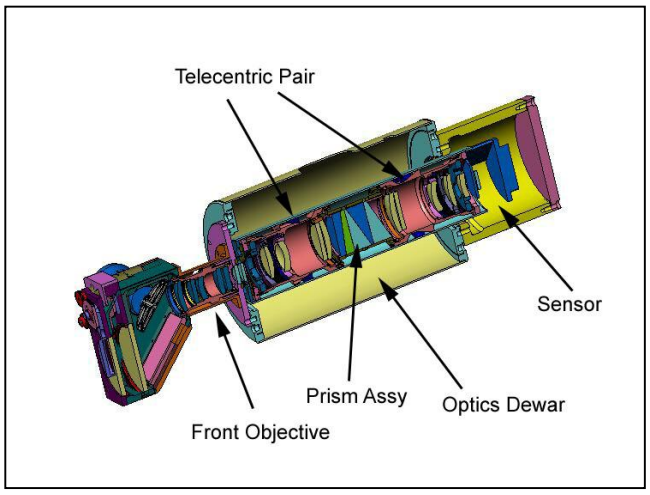

Figure 1: MWIR HSI

In order to achieve these goals, a system was designed based on a slit based optical system, with a prismatic dispersion element, passive athermalization, and a compact dewar (see Figure 1). The slit based system produces an image in one direction and spectral bands in the direction orthogonal to the slit. A scan mirror translates the image across the slit to provide a full frame hyperspectral image. Dispersion is provided by a multi-element prism. The entire system is cooled to cryogenic temperatures to reduce background noise.

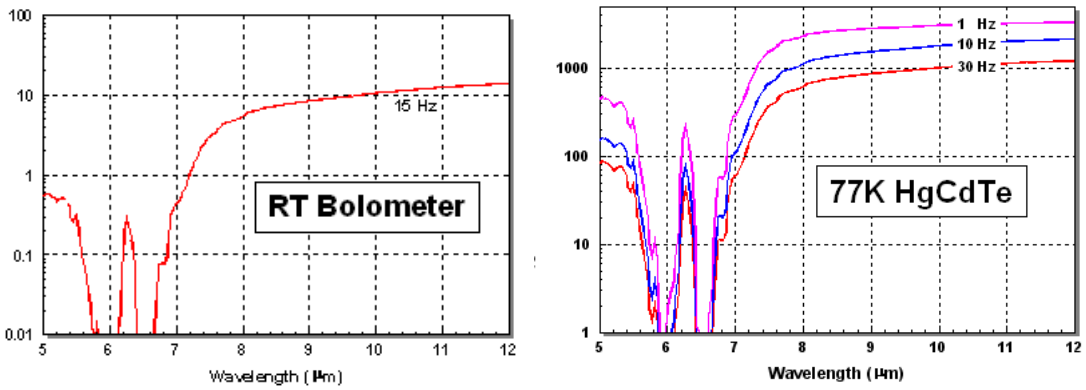

Figure 2: SNR of RT Bolometer and 77k HgCdTe FPA's

A key element in the system is the focal plane array (FPA). The hypercube consists of 256 x 256 pixels at 30 wavebands at 15 hypercubes/sec. The relatively narrow spectral bandwidth of each waveband will result in a very low intensity on the pixels of the FPA – approximately 3% of a broadband MWIR scene. This situation prevents the use of room temperature microbolometer arrays. Figure 2 shows the comparison of the SNR of a 300K blackbody scene viewed at various wavebands. For this application, the SNR for the cooled FPA is 100X to 1000X that of the uncooled technology.[2] In addition, a single detector technology that can be used for SWIR and LWIR wavebands inspired the use of a HgCdTe FPA.

Some of the major design challenges for this system include:

- Optical design of an F/1.75 achromatic, infinite conjugate

[2] F/1 optics, Frame Rate = Cubes/sec, 25 C Sunlit grass field, 100 m from Imager

- Achieving optical performance (passive athermalization, wavefront error, dispersion) at 77 K
- Cryogenic opto-mechanical design

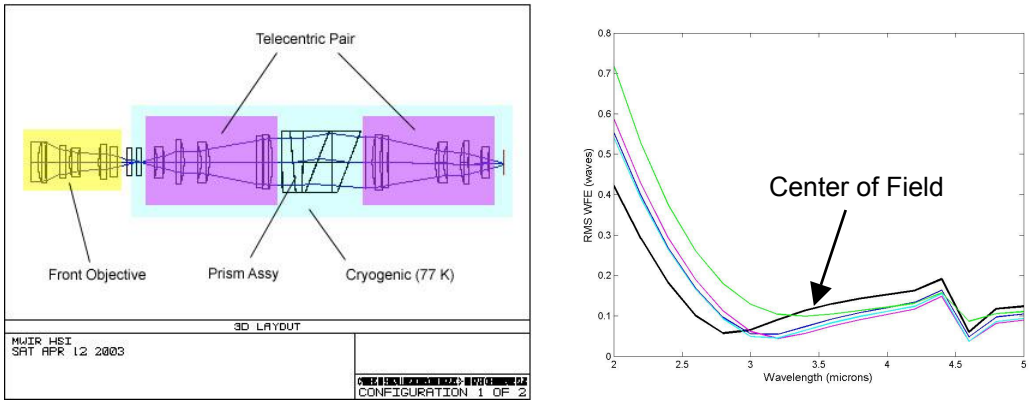

Figure 3: Optical Layout and Wavefront Error

The authors have reported on some of these challenges previously [3]. For summary purposes, the optical layout and wavefront error (WFE) of the system are shown in Figure 3.

3. MWIR HSI STATUS

Currently the MWIR HSI is being integrated and tested. The progress on integration includes redesign of the prism housing and optical testing of the infinite conjugates.

3.1 CRYOGENIC PRISM HOUSING

The prism housing is a critical component that provides the structural support, orientation, and spacing for the prism elements. The materials used in the prism (germanium, calcium fluoride, zinc selenide) are relatively fragile and brittle. In addition, the wavefront error requirements of the system are near diffraction limit. Given the number of elements in the system, the maximum allowable contribution from each element from cryogenic distortion is quite small ($WFE_{element}$ < λ/40 RMS). For these reasons, special attention was paid to the design of the prism holder.

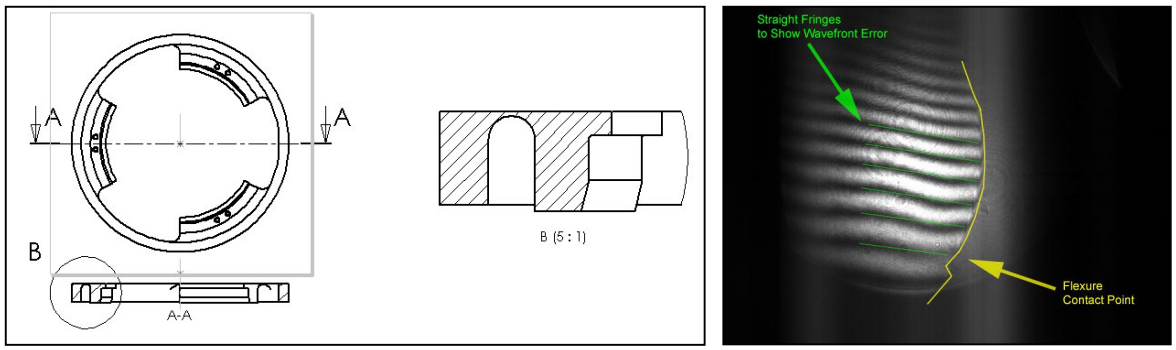

Figure 4: Lens Mount and Results for Stress Induced in Test Optic

In a previous publication [3], the opto-mechanical design of the lens holders was reviewed. These holders were designed with single blade flexures in a radial configuration (see Figure 4). Using shims, the stress on a test optic was measured and the peak-to-valley (PV) WFE was evaluated. Using this data as the criteria for maximum stress, a prism holder was designed to limit the stress on the prism elements below a critical value of 2 MPa.

Figure 5: Prism Assembly

The prism housing consisted of a load spreading bar suspended by flat springs that held the prism in a clam-shell cross-section tube (see Figure 5). The clam-shell only contacts the prisms along the bottom 30% of their circumference, removing the radial and hoop stress from the aluminum housing. Flat springs are used to provide a pre-load on a load spreading bar on the top of the prisms. The pre-load can be designed to hold the prisms with enough load to keep them from moving under several G's of acceleration without causing stresses that would affect the optical quality of the prisms.

To estimate the stress on the optic, first compliant springs are designed, then the displacement due to cryogenic strain is calculated, finally the force of the springs is calculated based on this displacement and distributed over the contact area of the load spreading bar.

Flat springs have a spring rate that can be estimated as:

$$F = kx = \frac{3E \times I}{l^3} x \rightarrow k = \frac{3E \times I}{l^3}, \quad I = \frac{1}{12} wh^3$$

where F is the force of the spring, x is the displacement of the spring, k is the spring rate, E (69GPa) is the modulus of the flat spring, I is the moment of inertia of the spring, l is the length (15 mm), w is the width (5 mm), and h is the thickness (1 mm) of the spring.

The displacement of the springs is merely the strain combined with the diameter of the housing:

$$\delta_{cryo} = \varepsilon_{cryo} \phi,$$

where ε_{cryo} is the strain (-3500 ppm) of the housing to cryogenic temperature and ϕ is the diameter of the housing (50 mm) and δ_{cryo} is the cryogenic displacement (175 μm).

Using this displacement, the force from each spring is: 1.5 N. Using six (6) springs, the total force would be 9 N. The contact area of the load spreading bar is roughly: 60 mm x 15 mm. The total stress should be on the order of 0.010 MPa.

The maximum stress level of the prism assembly is 1 – 2 MPa. This leaves a considerable margin that can be used to pre-load the prisms to prevent them from moving when the assembly is at room temperature. The mass of the prisms is approximately 0.33 kg. An acceleration of 10 G's would produce a force of 3.3 N. By machining a step on the bar, when a flat spring is clamped to the shell and the bar, it will be bent and exert a pre-load on the bar. This step height need only be 70 μm in order to hold the prisms at up to 10 G's.

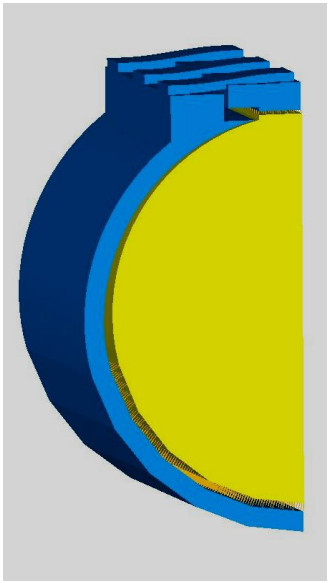

Figure 6: FEA of Prism Housing (Half-Plane Symmetry Exploited to Reduce Model Size)

In order to capture some of the more subtle effects of this design, a simple finite element model was constructed. The model (see Figure 6) was constructed with solid elements. The prisms were represented as a single glass element. The interface between the prisms and the housing was modeled with rigid bar elements. This relieved the hoop stress which would not normally be present in the actual housing. Exercising the model, the stress was computed as a function of radial distance (see Figure 7). Note that the stress is below the 2 MPa threshold over all of the clear aperture. In addition, the stress is extremely low over almost 90% of the clear aperture.

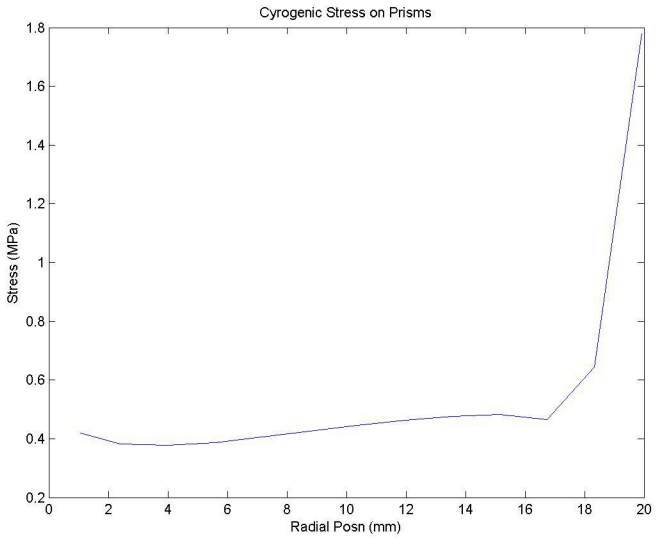

Figure 7: Stress on Prisms from Strain to Cryogenic Temperature (Max Allowed Stress = 2 MPa)

3.2 ROOM TEMPERATURE OPTICAL TESTING

The MWIR HSI optical system has 15 elements in the cryogenic section. With this many elements, it is prudent to test sub-sections of the optical system. The optical system can be separated into three (3) functional blocks: two infinite

conjugate lenses and a prismatic disperser. A single infinite conjugate was tested both at room temperature and at cryogenic temperature [3] and the performance was measured as diffraction limited. The most recent tests include: test of infinite conjugate pair and line spread function tests.

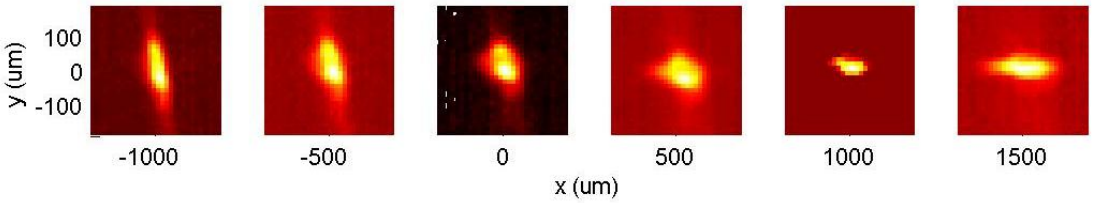

Figure 8: Through Focus Image of Crossed Slits (40 μm Square Aperture)

The two infinite conjugates were mounted and tested as a telecentric imaging pair. A slit was placed in the object plane and a slit rotated by 90 degrees was placed in the image plane. The image plane was relayed to a bolometer with 4:1 magnification and the system was illuminated by a blackbody source. Images of the focal spot through focus are shown in Figure 8. The slits were 40 μm in width. A perfect representation of the slits would be a 40 μm square. Convolving this 40 μm object with the predicted point spread function for the infinite conjugate pair results in an RMS spot radius comparable to the 60 μm measured with this technique.

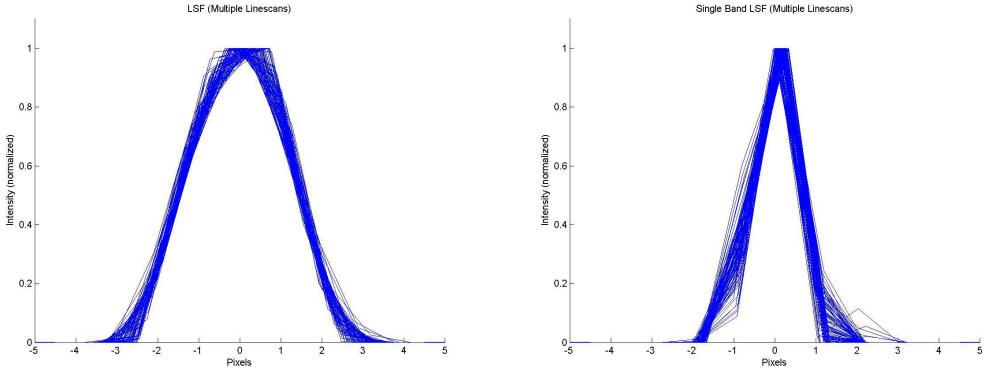

Figure 9: Line Spread Function for Broadband (left) and Narrow Band (right)

The line spread function was measured both broadband and line narrowed. The line spread function was evaluated using a slit in the object plane. The image was collected by the bolometer. Next, cross-sections of the line spread function were collected and a statistical RMS line width was calculated. Figure 9 shows the overlay of many of the cross-sections of the line spread function. The broadband line spread function is 2.4 pixel RMS width. However, the line spread function for narrow band illumination ($\Delta\lambda$ = 30 nm), the RMS width is 0.9 pixels.

4. ROOM TEMPERATURE HYPERSPECTRAL CUBES

Hyperspectral data was collected at room temperature to demonstrate spatial and spectral resolution. The system was configured with room temperature housings and a bolometer. Significant improvement in sensitivity and SNR are anticipated when the system is cooled and the HgCdTe FPA is used. Spatial resolution was demonstrated using a USAF Resolution target chrome pattern on a zinc selenide substrate. Spectral resolution was demonstrated using plastic films.

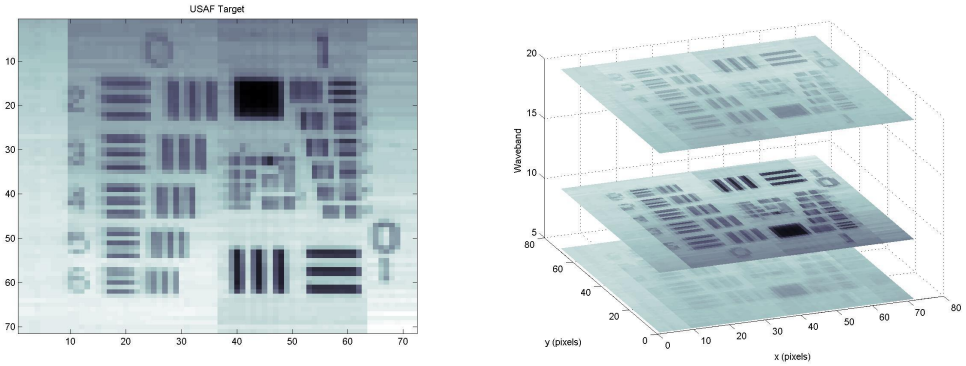

Figure 10: Hyperspectral Image of USAF Resolution Target

Figure 10 shows a hypercube for the USAF Resolution target. On the left is the image from a single spectral band demonstrating single pixel resolution. On the right, slices of the hypercube are shown. Images from three (3) of the wavebands are shown.

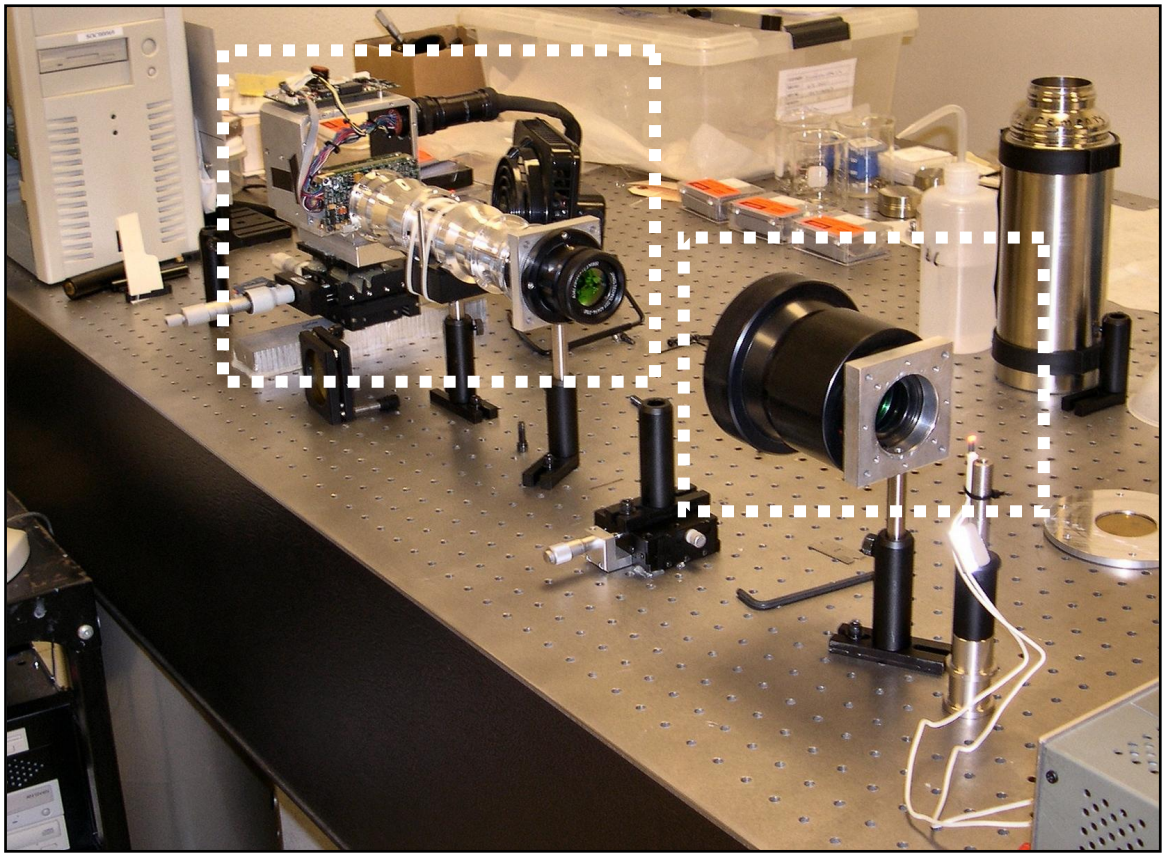

Figure 11: Hypercube Data Collection Test Setup

The MWIR HSI is not a thermal camera – it is a hyperspectral camera. As such, ideal objects to image have various spectral responses from 2 – 5 μm. The objects chosen were a series of plastic films were mounted on a single substrate. The films included varieties of kapton, polystyrene, and PET. In order to illuminate the sample, an infrared flashlight

was constructed. A filament was used as the blackbody source. This filament was collimated with a fast infrared lens (Janos ASIO f = 100 mm). The system is shown in Figure 11.

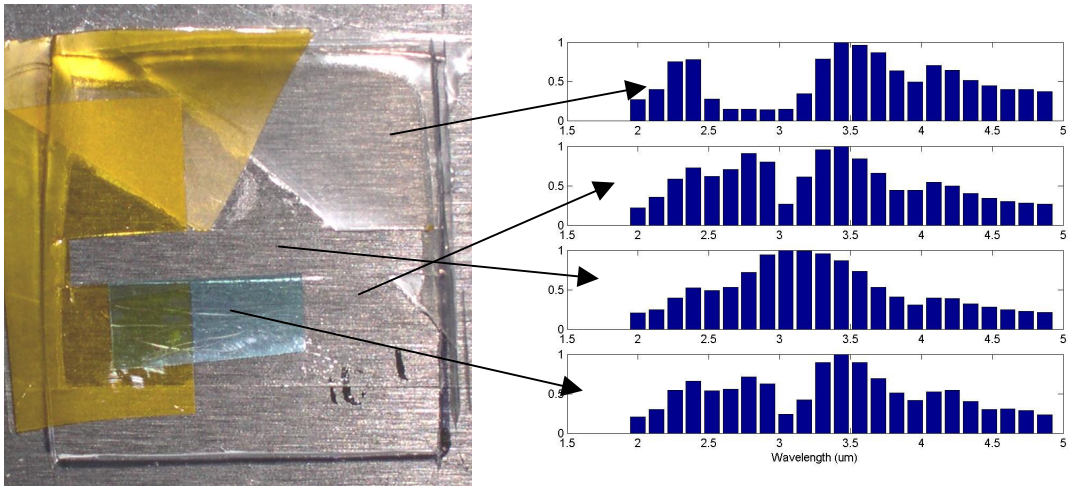

Figure 12: Plastic Film and Spectrum

The plastic film is shown in Figure 12 along with the spectrum from various portions of the image. The hypercube is shown in Figure 13 with several of the slices in the wavelength axis. The slices clearly indicate the various absorption spectrums of the different materials.

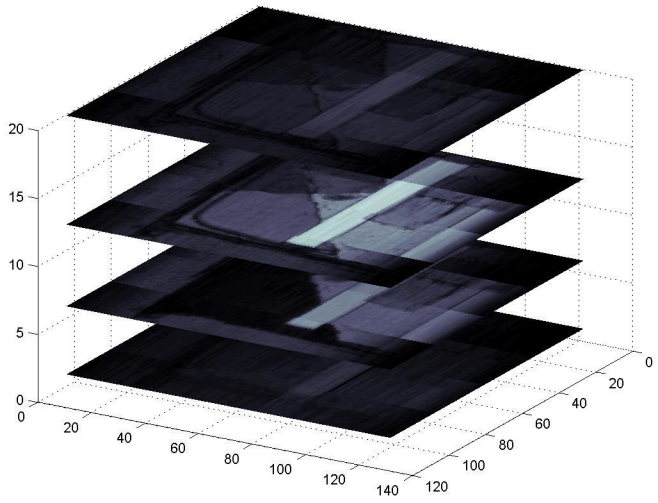

Figure 13: MWIR Hypercube for Plastic Film Sample

5. SUMMARY

In summary, a design for a MWIR hyperspectral imager has been described. Some of the optical and opto-mechanical design challenges have been detailed. A novel technique for mounting a prism assembly has been analyzed and optical performance data has been presented. Finally, hyperspectral data from the system has been collected. The results demonstrate the spatial resolution and spectral nature of the system.

6. REFERENCES

1. M. Dombrowski, J. Bajaj, and P. Willson, "Video-rate Visible to LWIR Hyperspectral Imaging and Image Exploitation," 31st Applied Imagery Pattern Recognition Workshop, October 2002.
2. M. Dombrowski, , P. Willson and C. LaBaw, "Performance and Application of Real-Time Hyperspectral Imaging," SPIE Imaging Spectrometry IV, Vol 3438, July 1998.
3. B. Catanzaro, M. Dombrowski, , P. Willson, J. Hendrixson, E. Hillenbrand and J. Wilcox, "Manufacturing and Performance Evaluation of a Refractive Real-Time MWIR Hyperspectral Imager," SPIE Infrared Technology and Applications XXIX, Vol 5074, April 2003.